The influence of calcium to phosphate ratio on the nucleation and crystallization of apatite glass-ceramics

A. CLIFFORD[1], R. HILL[1*], A. RAFFERTY[1], P. MOONEY[1], D. WOOD[2], B. SAMUNEVA[3], S. MATSUYA[4]
[1]*Department of Materials Science and Technology, University of Limerick, Limerick, Ireland*
[2]*Division of Restorative Dentistry, Leeds Dental Institute, University of Leeds, Clarendon Way, Leeds LS2 9LU, UK*
[3]*Higher Institute for Chemical Technology, Sofia 1756, Bulgaria*
[4]*Department of Dental Materials Engineering, Faculty of Dentistry, Kyushu University, Fukuoka 812 N 85 82, Japan*
E-mail: Robert.Hill@UL.IE

The nucleation and crystallization behavior of a series of glasses based on $4.5SiO_2$-$3Al_2O_3$-YP_2O_5-3CaO-$1.51CaF_2$ was studied. The parameter Y was varied to give calcium to phosphate ratios between one and two. All of the glasses studied crystallized firstly to fluorapatite ($Ca_5(PO_4)_3F$). The glass with a calcium to phosphate ratio of 1.67, corresponding to apatite, bulk nucleated to give fluorapatite (FAP). The glasses with calcium : phosphate ratios either less than that of apatite, or greater than that of apatite all exhibited surface nucleation of FAP. However, following a nucleation hold of one hour at approximately 50 K above the glass transition temperature these glasses exhibited bulk nucleation of FAP.

1. Introduction

Apatite-based materials are under intensive investigation for use as bone substitute materials [1]. Apatite materials are also attractive for dental applications. Most research has been directed towards the development of hydroxyapatite-(HA) based materials produced by a sintering route. However, there are considerable problems encountered on sintering HA, notably arising from degradation at high temperature. All the sintered HA materials lack sufficient strength and toughness. Furthermore, sintering is not an attractive route for the production of the complex shapes required for substitute bone parts and dental inlays. Subsequent machining using diamond-tipped tools would be required to form the intricate shapes needed. Such machining is often time consuming, expensive and difficult. Glass-ceramics are an attractive production route for producing apatite-based materials, offering the ability to cast components in the glassy state directly to the required shape. Near net shapes can be produced and the technique is suitable for the production of ''one off'' shapes. However, the most extensively studied glass-ceramic for potential use as a bone substitute material is the apatite-wollastonite (AW) system which can not be cast to shape and is processed by a sintering route [2]. Expensive diamond-tipped machining is again required to make the intricate shapes required for substitute bone parts. The AW system exhibits marked surface nucleation of both the apatite and wollastonite phases [2], and this is one of the reasons why materials based on this system are produced by a sintering route. The small glass particle size used for sintering restricts the growth of the crystalline phases and enables some limited control over the microstructure.

MacCulloch [3] first outlined the advantages of glass-ceramics in dentistry in the late 1960s. Grossman and coworkers [4, 5] developed the first castable glass-ceramic for dental use. This material, Dicor™ is based on a fluorosilicate glass and crystallizes to a fluormica phase. Dicor™ has insufficient strength and fracture toughness and is also prone to the formation of protoenstatite ($MgOSiO_2$) on the surface of the casting, which can cause excessive wear of the opposing dentition [6]. Hobo and Iwata [7], developed the castable AW system Cerapearl™ for dental crowns, but it suffered from uncontrolled surface nucleation during ceramming. They identified the advantage of having an apatite ceramic with a hardness close to that of natural enamel in preventing wear of the restoration and the opposing dentition, as well as the potential of using glass polyalkenoate cements for bonding the restoration to the tooth [7].

Recently Hill and co-workers [8–10] developed a readily castable glass-ceramic from the SiO_2-Al_2O_3-P_2O_5-CaO-CaF_2 system as a result of research

*Author to whom all correspondence should be addressed.

undertaken on ionomer glasses [11, 12] used in glass (ionomer) polyalkenoate cements. The high fluorite (CaF_2) content glasses of this system were shown to crystallize to fluorapatite and mullite and exhibited bulk nucleation, via prior amorphous phase separation [8–10]. Recently Dimitrova-Lukacs and Gllemot [13] have demonstrated that one of the compositions studied by Hill *et al*. [8], when cerammed, gives a material with high fracture toughness ($2.7\,MPa\sqrt{m}$) and high strength (260 MPa). Subsequently Clifford and Hill [10] confirmed that high fracture toughness values could be obtained. The high fracture toughness is thought to arise from the microstructure, which consists of interlocking apatite and mullite crystals. The apatite crystals can have an aspect ratio greater than 50 and during fracture these needle-like crystals are pulled out giving rise to a high fracture toughness. A typical interlocking apatite-mullite needle microstructure is shown in Fig. 1.

Frank *et al*. [14] have developed a pressable apatite glass-ceramic for dental crowns and inlays. The design of this new material allows it to be pressed to shape at 1150 °C, and consists of leucite and apatite phases.

Jana and Hoeland [15] and Hartman *et al*. [16] have investigated the crystallization of ionomer glasses, but no data is available on their nucleation behavior or their suitability for forming monolithic glass-ceramics. Furthermore, most of these studies are directed towards use of cerammed, or partially crystalline ionomer glass powders for use in polyalkenoate (ionomer) cement formation. Recently Moisescu *et al*. [17] studied the same glass compositions and produced glasses with anisotropic needle-like apatite crystals and high aspect ratios of up to 12 : 1. This should lead to glass-ceramics with improved mechanical strength. In a related study [18] it emerged that extrusion of partially crystalline samples at high temperatures led to the formation of apatite needles aligned with their crystallographic *c*-axis along the extrusion direction.

The original studies of Hill *et al*. [8] investigated a series of glasses based on: $1.5SiO_2$-Al_2O_3-$0.5P_2O_5$-CaO-$XCaF_2$ where X was varied between zero and one. The glass compositions studied do not evolve any significant amount of silicon tetrafluoride during melting as a result of carefully designing the glass composition, to ensure the fluorine atoms present are bound to the aluminum atoms of the glass network, rather than the silicon atoms [19]. Glass compositions with high fluorite contents and values of $X > 0.5$ were readily castable, underwent bulk cyrstal nucleation via prior amorphous phase separation and crystallized to fluorapatite and mullite. Compositions with low values of X $(X < 0.5)$ surface nucleated and crystallized to anorthite.

This series of glasses studied by Hill and co-workers [8–10] were poorly designed with both the calcium and the fluorine content being altered simultaneously as the proportion of fluorite (CaF_2) is altered. The Ca : P ratio which might be expected to influence the ability of these glasses to crystallize to apatite is altering as the value of X changes.

The objective of this paper is to investigate the influence of calcium to phosphate ratio of the glass on the nucleation and crystallization of glasses from the SiO_2-Al_2O_3-P_2O_5-CaO-CaF_2 system. A previous paper [20] has investigated the role of fluorine content on a series of glasses with a calcium to phosphate ratio of 1.67 corresponding to apatite. These glasses with the apatite stoichiometry exhibited two features that are undesirable in a practical glass-ceramic. They nucleated and crystallized too readily; the temperature difference between the glass transition temperature and the onset temperature for the first crystallization peak, Tp1 was typically less than 80 K resulting in these glasses being difficult to cast, without small amounts of crystallization occuring in large sections during the forming process. Secondly, it was found that glass compositions at the apatite stoichiometry, upon heat treatment, gave rise to numerous small $< 1\,\mu m$ apatite crystals, which did not coarsen readily to give the elongated crystals associated with high strength and toughness [10–13].

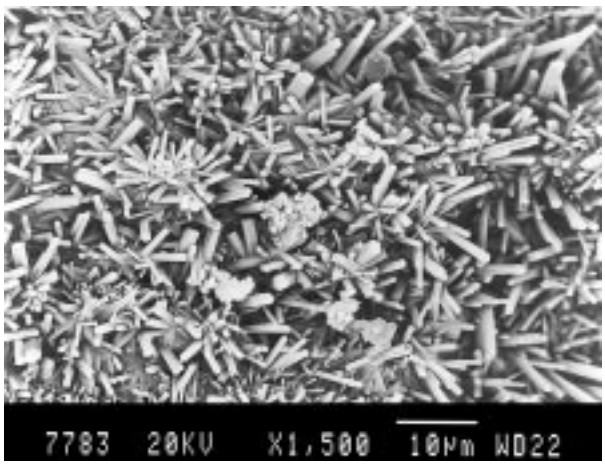

Figure 1 SEM of a fracture surface of an apatite-mullite glass-ceramic of composition $4.5SiO_2$-$3Al_2O_3$-$1.5P_2O_5$-3CaO-$2CaF_2$ heat treated to Tp2 exhibiting an interlocking microstructure.

2. Experimental

2.1. Glass design

In the present study the phosphate content was varied in the following series of glasses $4.5SiO_2$-$3Al_2O_3$-YP_2O_5-3CaO-$1.51CaF_2$. Crosslink densities were calculated using the approach outlined by Ray [22]. In this series of glasses the calcium to phosphate ratio is altered, while the crosslink density of the glass only varies slightly across the series from 1.31 to 1.34. All the glass compositions studied contain sufficient phosphorus and calcium, according to Lowenstein's rule [21], to allow the aluminum take up a four fold coordination state. Other glass criteria included ensuring the presence of at least one non-bridging oxygen per silicon, maintaining Al^{3+} in a four fold coordination state, and ensuring the fluorine content was less than the aluminum content in order to minimize SiF_4 volatilization during melting. This last criteria is based on the fact that an Si^{4+} cation will have a higher affinity for a non-bridging oxygen or O^{2-} anion that for a non-bridging fluorine or F anion, and that an Al^{3+} ion will bond the F anion, so preventing the formation of Si-F bonds in the glass network. The model is supported by MAS-NMR studies [23, 24] and by a trimethylsilylation analysis [25] of a previously studied

$2SiO_2Al_2O_3CaOCaF_2$ glass, which demonstrated the absence of Si-F bonds.

2.2. Glass synthesis

Glasses of defined chemical composition were synthesized for this study. The glasses were produced by melting the silica, alumina, phosphorus pentoxide, calcium carbonate, calcium fluoride and sodium carbonate in high density mullite crucibles (Zedmark Refractories, Earlsheaton, Dewsbury, UK) at a temperature of 1420 °C for 2 h. The resulting melts were rapidly shock quenched into water to prevent phase separation and crystallization. The glass frit produced was ground and sieved to give fine ($< 45\,\mu m$) and coarse (45–200 μm) particles, which were used in the subsequent analysis.

2.3. Glass characterization

2.3.1. Differential scanning calorimetry (DSC)

The glasses produced were characterized by differential scanning calorimetry using a Stanton Redcroft DSC 1500 (Rheometric Scientific, Epsom, UK). The crucibles used were matched pairs made of platinum-rhodium alloy. Alumina was used as the reference material. Runs were performed in dry nitrogen at a heating rate of 10 °C min^{-1} unless otherwise stated. The tendency of the glasses to undergo surface nucleation was assessed by performing DSC runs using three particle sizes; frit particles of 1–2 mm, coarse of 45–200 μm and fine of $< 45\,\mu m$.

Optimum nucleation temperatures were determined using the method outlined by Marrotta *et al*. [26] using one hour nucleation holds. Activation energies for crystallization were determined following nucleation holds at the previously determined optimum nucleation temperatures using the method outlined by Marrotta *et al*. [27], and the modified Kissinger method proposed by Matusita *et al*. [28]. The basis of the method developed by Marrotta *et al*. is

$$Ln\beta = Ec/RTp + \text{constant} \quad (1)$$

where β is the reciprocal of the heating rate, *Ec* is the activation energy of the process, *Tp* is the crystallization peak temperature and *R* the universal gas constant. Whilst the modified Kissinger method developed by Matusita *et al*. is based on.

$$Ln(Tp^2\alpha^n) = -mEc/RTp + \text{constant} \quad (2)$$

where *Tp* is the temperature corresponding to the maximum of the cystallization peak, *R* is the gas constant, α is the heating rate and in the modified Kissinger, *n* and *m* are the numerical constants, which depend on the crystallization mechanism. For the case of surface nucleation $n = m = 1$ whilst for bulk nucleation from a constant number of nuclei $n = m = 3$ whilst for bulk nucleation from an increasing number of nuclei $n = 4$ and $m = 3$.

These methods assume that the glass composition does not change as crystallization proceeds. This is questionable with glasses which are of different composition to the crystalline phase which forms. However, the activation energies obtained from these methods often give some insights into the nucleation and growth processes involved. Assumptions also have to be made with the modified Kissinger method concerning the appropriate values used for *n* and *m*. In some cases neither pure bulk nucleation or surface nucleation occur giving rise to non-integer values for *n* and *m*. Five heating rates of 2, 5, 10, 15 and 20 °C min^{-1} were used for the activation energy analysis.

2.3.2. Combined differential thermal analysis/thermal gravimetric analysis (DTA/TGA)

Combined DTA/TGA was used to study weight changes accompanying crystallization processes. A Stanton Redcroft DTA/TGA 1600 (Rheometric Scientific, Epsom, UK) was used with a flowing dry nitrogen atmosphere and a heating rate of 10 °C min^{-1}.

2.3.3. X-ray powder diffraction (XRD)

X-ray powder diffraction analysis was completed on heat treated glass samples for qualitative purposes. A Phillips powder diffractometer (Phillips Xpert diffractometer, Phillips, Eindhoven, NL) was used with Cu Kα X-rays. Every glass composition was heat treated using the tube furnace of the DSC to replicate the DSC analysis, using an identical heating rate, with samples taken at the individual crystallization temperatures for each glass.

2.3.4. Transmission electron microscopy

Transmission electron microscopy was carried out using a double replica procedure with replicas from cast samples. The carbon-platinum replicas were examined using a Phillips EM-400 electron microscope (Phillips, Eindhoven, NL).

2.3.5. MAS-NMR

MAS-NMR analyzes were conducted on ^{29}Si, ^{27}Al and ^{31}P nuclei at resonance frequencies of 79.50, 104.27 and 161.98 MHz, respectively, using an FT-NMR spectrometer (AM-400, Bruker, Germany). Spinning rates of the sample at a magic angle were 4 kHz for the ^{29}Si MAS-NMR and 5.5 kHz for the ^{27}Al and ^{31}PMAS-NMR. Recycle time was 30 sec for ^{29}Si and ^{31}P and 1 s for ^{27}Al. Reference materials for the chemical shift (in ppm) were tetramethylsilane for ^{29}Si, IM $AlCl_3$ for ^{27}Al and 85% H_3PO_4 for ^{31}P and their chemical shift was adjusted to zero ppm. Table I lists the ionomer glass samples studied using MAS-NMR.

3. Resulting and discussion

Three typical DSC traces are shown in Fig. 2 for glasses with Ca : P ratios of 2.0, 1.67 and 1.41. From Fig. 2 it can be seen that the glass transition temperature, Tg, does not change significantly across the series. This is expected on

TABLE I Ionomer glass samples studied using MAS–NMR

Sample	Description
A	Base glass (melt quenched into wear)
B	Base glass heated to 66 °C and held for 60 min
C	Glass annealed cast bar
D	Base glass heated to 66 °C (no hold)
E	Base glass heated to Tp1
F	Base glass heated to Tp2

TABLE II First peak crystallization temperature (Tp1) values for glasses in the series $4.5SiO_2$-$3Al_2O_3$-YP_2O_5-3CaO-$1.51CaF_2$

Glass	CLD	Ca : P	< 45 μm	Coarse	Frit
LG293	1.31	2.00	818	834	819
LG114	1.31	1.88	814	818	819
LG185	1.32	1.67	800	799	805
LG113	1.32	1.67	831	857	860
LG112	1.33	1.41	840	883	884
LG111	1.34	1.25	850	916	931
LG110	1.34	1.12	838	921	951

the grounds that the crosslink density of the glasses is almost constant. The values of the first peak crystallization temperature, Tp1 are given in Table II. It is apparent from Fig. 2 and Table II that the temperature difference between Tg and Tp1 increases dramatically for frit samples, as the calcium to phosphate ratio moves away from the apatite stoichiometry. This temperature window is important in that it facilitates the casting of large homogeneous glass monoliths.

XRD showed the first exotherm on the DSC trace to correspond to FAP (JCPDS powder diffraction file 15–876). Only broad diffuse diffraction lines corresponding to the most intense lines of synthetic FAP were found for glasses close to the apatite stoichiometry heat treated to Tp1. It is thought that a large number of small fluorapatite crystallites are formed, which give rise to pronounced X-ray line broadening in the diffraction pattern. On further heating these crystals coarsen giving rise to the characteristic FAP diffraction pattern. Frank *et al*. [14] observed a similar phenomena with leucite-apatite glass- ceramics. An XRD pattern for glass LG112 heat treated to Tp2 and 1200 °C is shown in Fig. 3.

The values for Tp1 are plotted against Ca : P ratio in Fig. 4 for the three different particle sizes of each glass. Surface crystallization, manifested by the increase in the value of Tp1 with increasing particle size is evident in all the glasses either side of the glass with the apatite stoichiometry of 1.67. The glass with the apatite stoichiometry also shows the minimum value for Tp1. Only the glass with the apatite stoichiometry undergoes bulk nucleation. The amount of structural rearrangement required for a glass composition to crystallize to FAP is likely to reach a minimum at a calcium to phosphate ratio of 1.67 and this explains the observed bulk crystal nucleation and the minimum value for Tp1 obtained. Wu *et al*. [29] studied the influence of calcium to phosphate ratio on apatite crystallization in MgO-CaO-Al_2O_3-SiO_2-P_2O_5 glasses. However these glasses contain no fluorine and the calcium to phosphate ratios were all above three and well above the apatite stoichiometry at 1.67. At such high Ca : P ratios the influence of Ca : P ratio on apatite nucleation and crystallization is likely to be less important. Zannotto and Muller [30] proposed that a glass composition which has a composition and molecular structure closely related to that of the crystalline phase will bulk nucleate and crystallize without large volume changes.

All the glasses with the exception of the glass with a Ca : P ratio of two exhibited two distinct exotherms on their DSC traces. The glass with a Ca : P ratio of two exhibited only one sharp exotherm for fine and coarse particles, but a second exotherm for frit samples. The second crystallization process, Tp2 shown in Table III generally increased in temperature with increasing particle size including a surface nucleated process. The exception to this phenomena was the apatite stoichiometry glass (LG185) which exhibited a second peak crystallization temperature which decreased in temperature with increasing particle size. The LG111 and LG110 glasses show the same characteristics on moving from coarse to frit. This phenomena is thought to be associated with the loss of volatile silicon tetrafluoride during the crystallization of the glass. A combined DTA/TGA trace is shown for glass LG185 in Fig. 5. The frit sample exhibits a negligible weight loss, whilst the fine sample exhibits a 1.6% weight loss. This weight loss starts to occur at a temperature corresponding to Tp1 onset. A commercial glass-ceramic Dicor™, which is based on a fluoro-silicate glass composition, has also been shown [31] to lose silicon tetrafluoride from its surface on

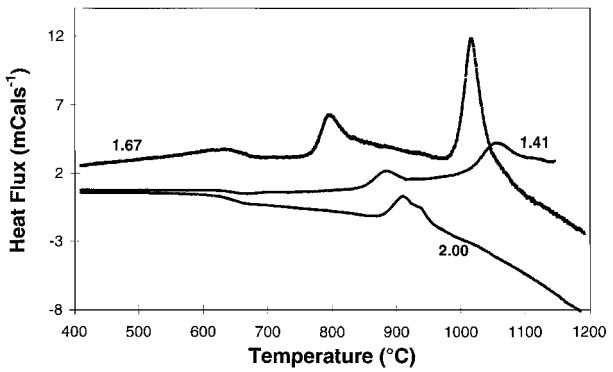

Figure 2 DSC trace for frit particles of glasses with Ca : P of 1.41, 1.67 and 2.00.

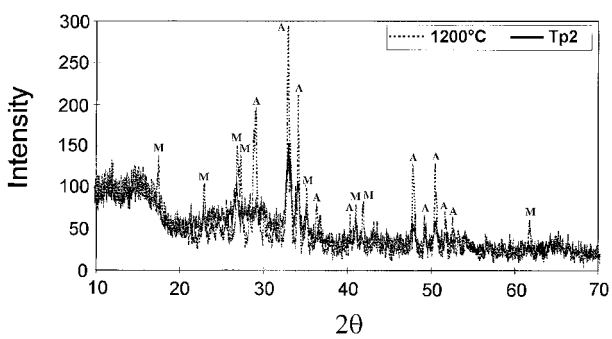

Figure 3 Overlapping XRD patterns for glass LG 112 heat treated to 1200 °C and T_{p2}. A = apatite and M = mullite.

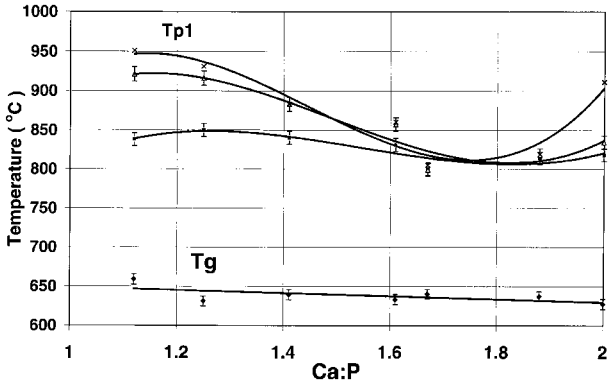

Figure 4 Plot of the glass transition temperature, Tg (◆) and first peak crystallization temperatures, Tp1 for frit (×), coarse (▲), and fine (■) glass particles plotted against calcium : phosphate ratio.

ceramming leading to the formation of protoenstatite ($MgO \cdot SiO_2$) at the surface, rather than the fluormica phase. The second crystallization process corresponded to mullite (JCPDS powder diffraction file 15–776) for the apatite stoichiometry glass, although significant quantities of anorthite (JCPDS powder diffraction file 12–301) were also found in heat treated samples in the calcium rich compositions (Ca : P $>$ 1.67). The berlinite form of $AlPO_4$ (JCPDS powder diffraction file 10–423) was found in the phosphate rich compositions (Ca : P $<$ 1.67). The proportion of anorthite increased with decreasing particle size suggesting anorthite is favored, either as a result of promotion of surface nucleation, or as a result of increased silicon tetrafluoride formation, arising from the increased glass surface area present. Anorthite has previously been shown to occur in glass compositions with calcium to phosphate ratios of 1.67 that contain no fluorine [20]. Previous DTA/TGA studies of fluoro-alumino-silicate glass compositions have shown weight losses accompanying crystallization [20, 32], and for this weight loss to disappear in fluorine free compositions.

Mullite, which is a high temperature refractory phase, is formed at unusually low temperatures. Mullite formation is thought to be favored following FAP crystallization since removing calcium and phosphate from the glass network in the form of FAP will cause an increase in the aluminum to silicon plus phosphate ratio above one, and will also result in insufficient Ca^{2+} and P^{5+} ions being available to charge balance the charge deficient Al^{3+} ion in a four coordinate environment. According to Lowenstein [21] this will force aluminum into higher five and six coordination states, thus favoring the formation of mullite in which aluminum is in a mixture of four and six coordinate states. Anorthite formation is likely to be favored by glass compositions in which the residual glass phase contains more calcium, since this will help maintain the aluminum in a four coordinate state. Glass samples with particle sizes below $>$ 45 μm undergo loss of silicon tetrafluoride upon crystallization resulting in a surface depleted in fluorine, which inhibits the crystallization of FAP, thereby favoring the formation of anorthite.

All the glasses either side of the apatite stoichiometry with Ca : P ratios between 1.41 and 1.88, and the glass at the apatite stoichiometry, exhibited well defined optimum nucleation temperatures just above the glass transition temperature. The optimum nucleation curves obtained using the Marrotta method [26] are shown in Fig. 6. All the glasses exhibited a nucleation maximum following a one hour temperature hold at between 20 and 60 K above the experimentally determined glass transition temperature. An optimum nucleation temperature just above the glass transition temperature is generally indicative of a nucleation process involving amorphous phase separation (APS). Two arguments exist [33] for explaining the role of APS in crystal nucleation in glass-ceramics. The first states that the barrier for homogenous crystal nucleation will be reduced, since the composition of one of the phase separated glass phases will be closer in composition to that of the crystal phase. The second emphasizes the importance of the creation of a large amount of internal surface for heterogenous crystal nucleation. Given that phase separation in related compositions [8–12, 15] is known to result in the formation of a calcium phosphate-rich glass phrase, the activation energy for crystallization will be reduced and the first argument is likely to apply. Though it must also be noted that heterogenous nucleation will also be favored.

Glass compositions with Ca : P $<$ 1.41 exhibited shallow optimum nucleation temperature curves that lacked a well defined nucleation maximum.

The activation energy for crystallization was determined for the first crystallization process corresponding to the formation of fluorapatite using both the Kissinger [27] and Matusita [28] methods, following nucleation holds. Activation energies were determined for all the glasses except the glass with a Ca : P ratio of 2.0. This glass was not studied since Tp1 corresponded to the crystallization of apatite, anorthite and mullite. Values for the exponents *n* and *m* of 3 and 3 were assumed in the Matusita *et al*. equation corresponding to bulk nucleation from a constant number of nucleii for samples with a

TABLE III Tp2 values for glasses in the series $4.5SiO_2$-$3Al_2$-YP_2O_5-3CaO-$1.51CaF_2$

Glass	Ca : P	$<$ 45 μm	Coarse	Frit
LG293	2.00	None	None	None
LG114	1.88	957	986	1001
LG185	1.67	1021	1005	983
LG113	1.61	958	999	1037
LG112	1.41	992	1045	1055
LG111	1.25	1033	1079	1055
LG110	1.12	1017	1065	1018

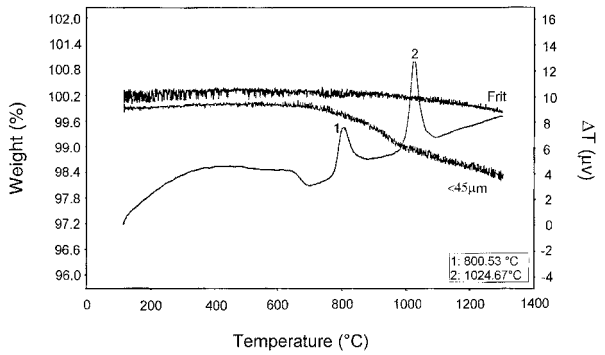

Figure 5 Combined DTA/TGA trace for the apatite stoichiometry glass with a Ca : P ratio of 1.67. The $< 45\,\mu m$ and frit DTA trace overlapped and for clarity only $< 45\,\mu m$ trace is shown.

nucleation hold and values of 4 and 3 without a nucleation hold. The data is shown in Table IV and Fig. 7. There was good agreement between the Kissinger and Matusita methods for all the glasses with a nucleation hold confirming the assumption of values of 3 and 3. It was expected that the glass with the calcium to phosphate ratio corresponding to that of FAP would have the lowest activation energy for crystallization, but this proved not to be the case. Glasses with slightly higher and lower calcium to phosphate ratios than 1.67 exhibited significantly lower activation energies. The Matusita plot without a nucleation hold exhibited some curvature for LG185, which was thought to arise from a mixed mode behavior, with some surface nucleation occuring at high heating rates. The faster heating rates are likely to suppress the APS process by providing too little time for it to occur. There was also marked disparity between the Matusita and Kissinger values for the activation energies obtained. The activation energies were therefore repeated with a nucleation hold to try and eliminate the contribution from surface nucleation at high heating rates.

The good agreement between the Kissinger [27] and Matusita [28] methods for all the glasses following a nucleation hold supports the assumptions concerning the nucleation mechanism made with the Matusita method.

The optimum nucleation temperature determined using the Marrotta method did not show a minimum at the apatite stoichiometry, which corresponded to a minimum in the first peak crystallization temperature. The activation energy for crystallization obtained using the Matusita and Kissinger methods also did not show a minimum at the apatite stoichiometry, but became smaller with reducing calcium to phosphate ratio. It is plausible that once nucleation is achieved the rate determining step for cystallization corresponds to the crystal growth step and the ease with which the glass network can be rearranged to give fluorapatite. The activation energy for crystallization may, therefore, correspond to the activation energy for viscous flow and this would be expected to decrease with an increase in the proportion of phosphate in the glass network. This is due to the phosphorus-oxygen bond strength being considerably weaker than that of the silicon-oxygen or aluminum-oxygen bond strengths.

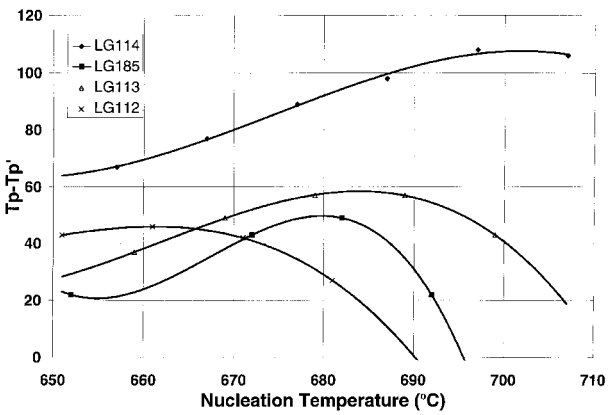

Figure 6 Optimum nucleation curves for glasses with varying Ca : P ◆ = 1.88, ■ = 1.67, ▲ = 1.61 and × = 1.41.

Likitvanichkal and La Course [34] determined the activation energy of apatite crystallization as being 514 ± 57 and 482 ± 36 KJ mol^{-1} respectively, for coarse and fine particles in the AW glass-ceramic composition. The values obtained in the present study are generally lower, however this is to be expected on the grounds that the activation energy for crystallization often correlates with that for viscous flow. These glasses have a much higher fluorine content and are more disrupted glasses and would therefore be likely to have lower activation energies for viscous flow and crystallization.

Transmission electron microscopy using a carbon-platinum replica technique demonstrated strong evidence of amorphous phase separation giving rise to an interconnected structure in LG113 after a nucleation hold. The microstructure of the LG113 glass following a one hour heat treatment at Tp1 is shown in Fig. 8; crystals and the remains of an interconnected structure are visible. The crystal sizes vary from 0.4 to 0.8 μm. Related glass compositions also demonstrated evidence of APS and interconnected structures [8–12, 15].

MAS-NMR studies were carried out on the glass with Ca : P = 1.41 to obtain structural information regarding the glass phase during the heat treatment. These studies were conducted on the coarse glass, the cast glass and on a sample of coarse glass heat treated to the optimum nucleation temperature of 661 °C for one hour. Also for the glass heat treated to Tp1, for the glass heat treated to (Tp1 + Tp2)/2 and for the glass heat treated to Tp2. Table IV lists the heat-treatment details for these samples.

The ^{29}Si, ^{27}Al and ^{31}P spectra of the glasses are shown in Figs. 9 to 11 respectively. The silicon spectrum shows a broad peak at -90 ppm that shifts slightly in the negative direction as the heat treatment proceeds. The peak width is slightly larger in the heat treated glass than the original one. The chemical shift observed depends on both the number of bridging oxygen (m) per SiO_4 unit and the number of aluminum (n) connected by oxygen with the SiO_4unit. When a structural unit of the aluminosilicate glass network is expressed as $Si(OSi)_{m-n}(OAl-)_n(O-)_{4-m,}(Q_m(_nAl))$, the chemical shift increases with decreasing m or increasing n [35]. It is reported that chemical shift of Q4 (3A1), Q4 (4A1) and Q3 (OA1) are -90 ppm, -88 ppm and -90 ppm [35]. This glass probably contains these species, though it is difficult to determine the exact distribution of these

TABLE IV Optimum nucleation temperatures and activation energies for crystallization determined by the Matusita and Kissinger Methods

Glass	Ca : P	Tg(°C)	Optimum nucleation temperature (°C)	Matusita, Ea ($KJmol^{-1}$)	n	m	Kissinger Ea ($KJmol^{-1}$)
LG114	1.88	637	687	475	3	3	464
LG185	1.67	640	682	684	3	3	673
LG185	1.67	640	No Hold	393	4	3	163
LG113	1.61	640	675	410	3	3	398
LG112	1.41	641	661	362	3	3	350
			No Hold	325	3	4	229
LG111	1.25	649	670	333	3	3	320
LG110	1.12	640	700	352	3	3	339

species from the chemical shift. As already described, the peak width becomes broader and moves in a more negative direction in chemical shift after the heat treatment. This indicates an increase in m and/or a decrease in n. Crystallization of fluorapatite causes the removal of network modifying Ca^{2+} ion from the glass network and will increase the number of bridging oxygen. The heat treatment also causes a preferential bonding of the Al^{3+} ion with PO_4^{3-} ion as described later.

The aluminum spectra (Fig. 10) show a broad resonance for all the samples except for the sample heat treated to Tp2; this shows a sharp peak at approximately -39 ppm. The chemical shift value is in the range for aluminum in a four coordinate state, but is low compared with that of the oxide or in glasses. It was suspected that it corresponded to $AlPO_4$. The spectra for $AlPO_4$ with a trydymite crystal structure was run and the aluminum resonance matched that in the glass heat treated to Tp2. Dollase *et al*. [35] reported a value of -41 ppm close to -39 ppm with a resonance frequency of 78.206 MHz and a MAS rate of 4 KHz.

The glass heat treated to (Tp1 + Tp2)/2 shows a sharp resonance at 2 ppm in the ^{31}P spectra (Fig. 11), which corresponds with phosphorus in a crystalline orthophosphate environment. A previous study [16] has shown that the ^{31}P chemical shift in apatite is independent of fluorine content and is at 2 ± 0.3 ppm. This resonance is stronger in the glass heat treated to Tp2 indicating that the volume fraction of apatite crystals is growing with increased temperature and time. There are also two side bands at around -29 ppm and -34 ppm. In the spectra obtained at different MAS rates, the side bands are shifted, while a small peak is still present at approximately -29 ppm. The peak at -29 ppm corresponds well with that found by Dollase *et al*. [35] for PO_4 in $AlPO_4$. Dollase *et al*. [35] found a shift of -28 ppm and noted that the chemical shift depended on the number of Al atoms surrounding a PO_4^{3-} tetrahedron. Semi-quantitative X-ray powder diffraction found fluorapatite (53%), anorthite (20.6%), $AlPO_4$ (15%), and mullite (12%). There is still some phosphorus in the glass phase following crystallization of fluorapatite. The broad peak at around -10 ppm in the glasses heat treated to temperatures above Tp1 shifted in a negative direction as the heat treatment temperature increased. This suggests that the number of A1 atoms coordinating around a PO_4^{3-} tetrahedron is increasing with heat treatment and indicates that there are $AlPO_4$ type species in the residual glass phase. This is to be expected given the fact that the Ca : P ratio of this glass is less than 1.67, i.e. on the phosphate-rich side of the apatite stoichiometry. It was

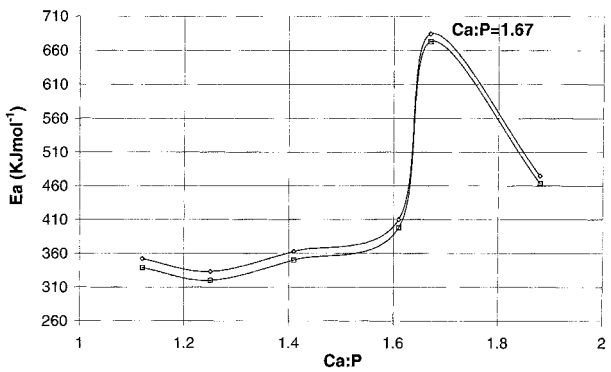

Figure 7 Activation energy for crystallization plotted against Ca : P ratio of the glass, using Kissinger (bottom curve) and Matusita (top curve) methods.

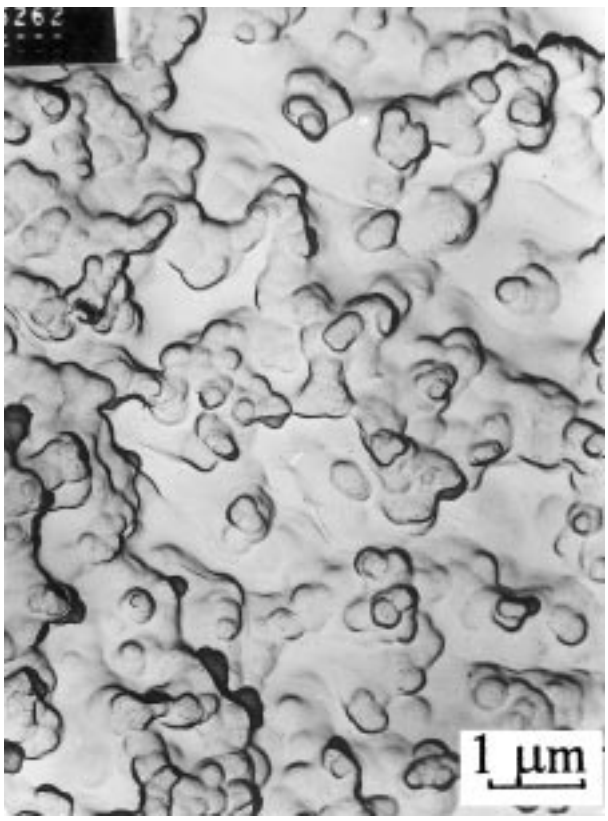

Figure 8 TEM (of the LG113 glass heat treated for 1 at Tp1. Note the presence of crystals and the remain of an interconnected structure.

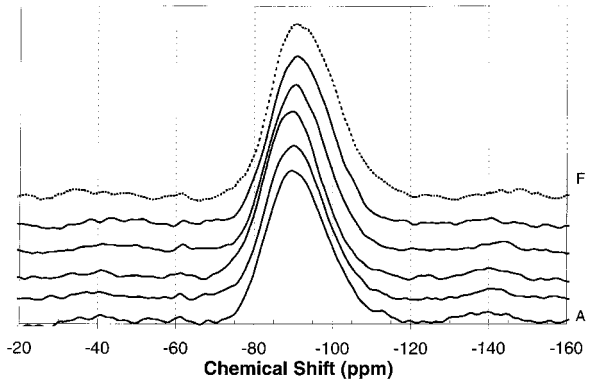

Figure 9 ^{29}Si MAS-NMR spectra for the glass with a Ca : P ratio of 1.41.

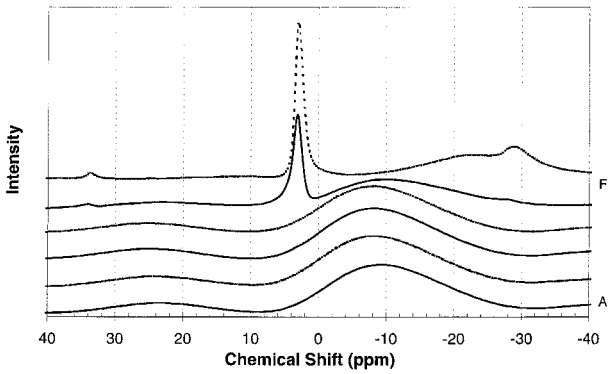

Figure 11 ^{31}P MAS-NMR spectra for the glass with a Ca : P ratio of 1.41.

expected that there would be a change in the ^{31}P MAS-NMR spectrum of the glass heat treated for one hour at the optimum nucleation temperature, consistent with the formation of a calcium phosphate-rich glass phase. Though the change in chemical shift is quite small, the peak seems to shift slightly in a more positive direction after the heat treatment. Most calcium orthophosphate compounds show a positive chemical shift around 0 ppm in their ^{31}P MAS-NMR spectra [16]. The observed shift in the peak may be caused by the phase separation of a calcium phosphate-rich glass phase. However, considering that the change in shift is quite small, the as-quenched glass may already be phase separated on an atomic scale and that heat treatments above the glass transition temperature result in a coarsening of the microstructure. Nucleation of the apatite phase may be promoted as a result of the size of the calcium phosphate domains increasing above the critical size required for apatite crystal nucleation.

4. Conclusions

The calcium to phosphate ratio of the glass has a significant influence on the nucleation and cystallization behavior. A calcium to phosphate ratio close to 1.67 favors bulk nucleation of fluorapatite. Compositions close to the apatite stoichiometry exhibited surface nucleation, but could be made to bulk nucleation by holding for one hour in the vicinity of the glass transition temperature. Holding at a temperature close to the glass transition allows time for amorphous phase separation to occur which either creates internal surface for nucleation to take place or reduces the activation energy for nucleation as a result of the composition change following amorphous phase separation.

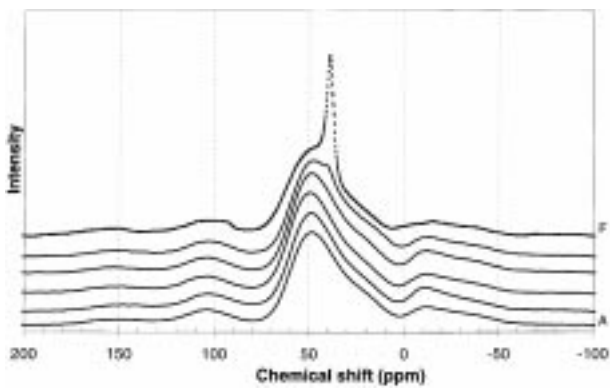

Figure 10 ^{27}AL MAS-NMR spectra for the glass with a Ca : P ratio of 1.41.

Acknowledgments

The authors would like to acknowledge the funding from the European Union COPERNICUS scheme Contract CIPA-CT94–0145.

References

1. R. D. RAWLINGS, *Clincal Material* **14** (1193) 155.
2. T. KOKUBO, S. ITO and S. SAKKA, *J. Mater. Sci.* **21** (1986) 535.
3. W. T. MACCULLOCH, *Br. Dent. J.* **124** (1968) 361.
4. D. G. GROSSMAN, in ''Cleation and Crystallisation in Glasses'' (American Ceramic Society Inc., Ohio, 1952) p. 249.
5. P. J. ADAIR and D. G. GROSSMAN, *Int. J. Periodont. Rest. Dent.* **2** (1984) 33.
6. S. D. CAMPBELL and J. R. KELLY, *Int. J. Prosthodont.* **2** (1989) 459.
7. S. HOBO and T. IWATA, *Quintessence Int.* **16** (1985) 207.
8. R. G. HILL, PATEL and D. J. WOOD ''Preliminary Studies on Castable Apatite-Mullite Glass Ceramics'' in *Bioceramics*, 4, edited by W. Bonfield, G. W. Hastings and K. E. Tanner, (Butterworth-Heinemann, London, 1991) pp. 79–86.
9. R. HILL and D. WOOD, *J. Mater. Sci. Mater. Med.* **6** (1995) 311.
10. A. CLIFFORD and R. HILL, *J. Non. Cryst. Solids.* **196** (1996) 346
11. D. WOOD and R. HILL, *Biometerials* **12** (1991) 164.
12. R. G. HILL, C. GOAT and D. WOOD, *J. Amer. Ceram. Soc.* **75** (1992) 778.
13. M. DIMITROVA-LUKACS, L. GILLEMOT, ''Bioactive-Bioinert Composite Bioceramics'' in Third Euroceramics, **3,** edited by P. Duran and J. F. Fernandez (Faenza Editrice Iberica S.L. Spain, 1993) pp. 179–84.
14. M. FRANK, M. SCHWEIGER, V. RHEINBERGER and W. HOELAND, ''Leucite Containing Phosphosilicate Glass-Ceramics,'' US patent, No. 5,698,019, Dec 16, 1997.
15. C. JANA and W. HOELAND, *Silicates Industriels*, **56** (1991) 215.
16. P. HARTMANN, C. JANA and M. BRAUN, *J. Mater. Sci.: Mater. Med.* **6** (1995) 150.
17. C. MOISESCU, C. JANA and C. RÜSSEL, *J. Non. Cryst. Solids.* **248** (1999) 169.
18. C. MOISESCU, C. JANA, S. HABELITZ, G. CARL and C. RÜSSEL, **248** (1999) 176.
19. E. DE BARRA, Ph.D. Thesis, University of Limerick, 1997.
20. A. RAFFERTY, A. CLIFFORD, R. HILL, D. WOOD, B. SAMUNEVA and M. DIMITROVA-LUKACS, *Amer. Ceram, Soc.*, to be published.

21. W. LOWENSTEIN, *Am. Miner.* **39** (1954) 92.
22. N. H. RAY in ''Organic Polymers'' (Academic Press, London, 1978).
23. N. H. MOHIALDIN, MSc. Thesis, University of Greenwich, 1996.
24. S. C. KOHN, R. DUPREE, M. G. MORTUZA and C. M. B. HENDERSON, *Am. Miner.* **76** (119) 3109.
25. R. G. HILL, D. J. WOOD and M. THOMAS, *J. Mater. Sci.* **34** (1999) 1767.
26. A. MARROTTA, A. BURI and F. BRANDA, *ibid.* **16** (1981) 341
27. A. MARROTTA, A. BURI, F. BRANDA and S. SAILLO, ''Nucleation and Crystallisation in Glasses'' (American Ceramic Society Inc Ohio, 1982) pp. 145–152.
28. K. MATUSITA, S. SAKKA and Y. MATSUI, *J. Mater. Sci.* **10** (1975) 961.
29. S. WU, C. L. WANG and M. HON, *J. Ceram. Soc. Japan* **103** (1995) 99.
30. E. ZANNOTTO and E. MULLER, ''Physics of Non-Crystalline Solids'' Taylor and Francis, London, 1992).
31. D. J. WOOD, N. L. BUBB, A. CLIFFORD, R. G. HILL and J. C. KNOWLES, *J. Mater. Sci. Lett.* **18** (1999) 1001.
32. A. RAFFERTY, A. CLIFFORD, R. HILL, D. WOOD, B. SAMUENVA and M. DIMITROVA-LUKACS preparation. in,
33. P. F. JAMES GLASSES and ''Glass-ceramics'' (Chapman and Hall, London, 1989) p. 59.
34. S. LIKITVANICHKAL and W. C. LA COURSE, *J. Mater. Sci.* **33** (1998) 5001.
35. W. A. DOLLASE, L. H. MERUIN and A. SETALD, *J. Solid State Chem.* **83** (1989) 140.
36. G. ENGELHARDT, M. NOFZ, K. FORKEL, F. G. WISHMANN, M. MAGI, A. SAMOSON and E. LIPPMAA, *Phys. Chem. Glasses*, **26** 5 (1985) 157.

Received 24 August
and accepted 13 December 1999